Desalination and Water Treatment
www.deswater.com

doi: 10.1080/19443994.2013.821034

52 (2014) 6505–6518
October

Taylor & Francis
Taylor & Francis Group

Phenol removal from aqueous phase by adsorption on activated carbon prepared from paper mill sludge

Kasra Pirzadeh, Ali Asghar Ghoreyshi*

Chemical Engineering Department, Babol University of Technology, Shariati Street, Babol, Iran
Tel. /Fax: +98 111 3234204; email: aa_ghoreyshi@nit.ac.ir

Received 16 March 2013; Accepted 5 June 2013

ABSTRACT

A new activated carbon was synthesized using paper mill sludge as a low cost waste material. It was employed to remove phenol from aqueous solution in the concentration range of 0–60 mg/l and temperature range of 25–45˚C. The adsorbent characteristics were determined by different analyses such as BET, FTIR, and SEM. The effects of pH, adsorbent dosage, initial phenol concentration, contact time, and temperature on phenol adsorption were investigated. The maximum adsorption capacity of 15.04 mg/g was obtained at optimum condition. The equilibrium experimental data were analyzed by several model isotherms. The best-fitted adsorption models were found to be in the order: Langmuir–Freundlich > Freundlich > Langmuir. The kinetics of phenol adsorption was investigated using different kinetics models. Experimental kinetic data were well described by the pseudo-second-order model. It was found that the temperature had negative impact on the phenol removal. Thermodynamic parameters such as Gibbs free energy, the enthalpy, and the entropy changes were determined. The results indicated that phenol adsorption process was spontaneous, exothermic, and controlled by physical sorption mechanism. Finally, the results revealed that the paper mill sludge can be employed as a promising raw material in terms of economical and technical aspects for the removal of contaminants from wastewaters.

Keywords: Paper mill sludge; Phenol; Activated carbon; Adsorption; Isotherm; Kinetics

1. Introduction

In recent years, water pollution has become a major risk, especially in developing countries, due to insufficient funds that are accessible for wastewater treatment. At present, existence of organic pollutants is more dangerous than inorganic ones due to their potential mutagenicity, carcinogenicity, and toxicity [1]. Moreover, they cause an unpleasant effect on odor, taste, and color of drinking water. Phenol and its derivatives are one of the hazardous organic pollutants.

Phenolic compounds are considered as major pollutants, since they are harmful for living creatures even at low concentration and many of them have been classified as hazardous contaminants due to their potential harm to environment [2]. The main sources of phenol and its derivatives which pollute the aquatic environment are wastewaters from paint, pesticide, coal conversion, polymeric resins, steel, petroleum, and petrochemical industries [3]. Phenol could have

---

*Corresponding author.

1944-3994/1944-3986

serious effect on human health, it may cause malfunction in brain, digestive system, eye, heart, liver, lung, and skin [4]. On the basis of these problems, strict legislation has been enacted for discharging phenolic contaminants to environment and thus this makes it necessary to develop an effective technique to remove them from wastewater [5]. There are several techniques for phenol removal such as oxidation, biodegradation, chemical coagulation, incineration, reverse osmosis, and adsorption. All the above mentioned methods have some advantages; however, high energy consumption, low selectivity, and high operational costs have restricted their applications [6]. Among these techniques, adsorption is one of the most effective one either in laboratory or industrial scale [7].

Adsorption occurs due to the affinity of an adsorbent for adsorbate species. Adsorption process continues till the equilibrium is achieved between the species bounded to the adsorbent and those remaining in the solution [8]. Activated carbon is a carbonaceous material which has a porous structure that turns it to a superior adsorbent [9]. Due to its high adsorption capacity, activated carbons have been used in mixture separation and liquid purification [10]. Activated carbon can be produced from any carbonaceous material through physical and chemical activation. Characteristics of porosity in activated carbon including pore size distribution, pore shape, and surface chemistry can be affected by the nature of the precursor, activation method, and activation conditions. Physical activation is a two-step process; in the first step, the material is carbonized under inert atmosphere and in the second step, the carbonized material is activated at high temperature using steam or carbon dioxide as an activating agent in order to develop porous structure. In chemical activation, the precursor is impregnated with activation reagent and then heated in inert atmosphere. Dehydration and oxidation reactions of chemicals led to pore development. Then, the produced char is washed to remove residual impurities [11]. In comparison to physical activation, chemical activation has some advantages: low energy and operating cost, high carbon yields, and high surface area with porous structure [12,13]. However, high cost of production and regeneration associated with these kinds of activated carbons are disadvantages that may restrict their applications [14]. Thus, there is a growing demand to find out an adsorbent, not only being easily available and relatively effective but also have a low cost for adsorption of contaminants from effluents. Generally, adsorbents with little processing, plentiful in the nature or waste residues generated from industries are considered as low cost adsorbents [15]. The low cost adsorbent can be prepared from agriculture waste materials such as rice husk [16], pine bark [17], nutshells [18], olive stone [19], and sugarcane bagasse [20].

Nowadays, industrialization and urbanization have increased disposal of industrial and municipal wastewaters to the environment. This poses a major environmental problem because hazardous contaminants available in wastewaters are non-biodegradable and resists to conventional biological treatment, so that removal of contaminants from wastewaters are difficult [21]. Sewage sludge is a biomass which is produced in a large amount from biological activities of municipal wastewater treatment plants and industrial wastewaters. Because of the rapid growth in population, disposal of sewage sludge has become a great concern in the recent years. There are several ways to dispose sewage sludge including landfilling, incineration, and sea dumping [22]. Because of rapid urbanization, finding appropriate land for landfilling is becoming challenging task. Sea dumping is banned in many countries due to pollution caused by oil, fats, and other undesired compounds. Incineration method used in many countries is becoming restricted due to legislations enacted for greenhouse gas emissions and also for energy consumption. Considering these problems, lots of efforts were made by many investigators to find out a way for reusing sewage sludge instead of disposing them. Activated carbon produced during aerobic treatment of different industrial wastewaters is a suitable precursor for the production of activated carbon, since it contains enough carbon in its structure. This approach not only reduces the amount of sewage sludge, but also converts this waste to useful material such as biosorbent for wastewater treatment [23]. Although the paper mill sludge was previously used to synthesize activated carbon [24], its application for phenol removal has not been reported in the literature. The novelty of the present work lies in using paper mill sludge-based activated carbon for phenol removal that has shown a remarkable adsorption capacity.

The main aim of the present study was to synthesize a new adsorbent from low cost carbonaceous material obtained from the treatment of pulp industry wastewater. Then, the efficiency of the synthesized adsorbent for removal of phenol from aqueous solutions was investigated through the equilibrium and kinetic studies in batch system. The optimum conditions to attain maximum adsorption capacity were determined by the examination of different parameters affecting on adsorption. Theoretical interpretations of the experimental data were carried out in terms of equilibrium isotherm and kinetic models.

Also, thermodynamic analysis was performed to evaluate the adsorption thermal nature and degree of randomness with respect to the values obtained for enthalpy and entropy of adsorption.

2. Materials and methods

2.1. Preparation of activated carbon

Paper mill sludge was collected from the pulp and paper plant, Chouka, Talesh, in north of Iran. The raw paper mill sludge was dried in an oven at 110°C for 24 h and crushed mechanically using a blender, then sieved to particle size of 0.3 mm. A 20 g of dried sludge was impregnated in 250 ml of 1.2 M $ZnCl_2$ with impregnation ratio of 2:1 at 80°C for 8 h. Then, the slurry was dried out at 110°C for 24 h and subsequently pyrolyzed in a stationary horizontal furnace under a pure nitrogen gas atmosphere; the heating rate was kept at 15°C/min. The pyrolyzing temperature and dwelling time were 700°C and 1 h, respectively. Following pyrolysis, the product was washed with 0.1 M HCl to remove residual compounds and then rinsed with distilled water to adjust the pH around the neutral level (pH = 7) and then dried at 110°C for 12 h.

2.2. Characterization of the paper mill sludge-based activated carbon

Elemental analysis of paper mill sludge was carried out (Costech ECS 4010, USA) to find out the amount of elements such as C, N, etc. The surface morphology was observed by scanning electron microscopy (SEM, KYKY-EM3200, China). The Fourier transform infrared spectroscopy (FTIR) was performed on a Tensor-27 (Bruker, Germany) spectrum. For spectroscopic characterization of the precursors, a specified amount of samples was completely mixed with KBr (FTIR grade, Merck) keeping 1:100 ratio (w/w). Transmission measurements were performed in the 400–4,000 cm^{-1} region. The specific surface area was measured using physical adsorption of N_2 at 77 K in Belsorp mini II apparatus (Bel-Japan Company). The surface area was estimated using Brunauer–Emmett–Teller (BET) method.

2.3. Batch adsorption experiments

Stock solution of phenol was prepared by dissolving a certain amount of phenol in distilled water. 150 ml of phenol solution with known initial concentration was added to the specified amount of adsorbent in 250 ml stoppered Erlenmeyer flasks at each experimental run. The flask was placed in an orbital shaker (IKA, KS 4000i control) running at 180 rpm and constant temperature. Samples were collected periodically at each 0.5 h time interval to determine solution concentration until the equilibrium (after 20 min) was reached. Before analysis, the samples were filtered in order to minimize the interference of carbon fines with the analysis. The concentration of the solution was determined using the spectrophotometer (2,100 SERIES, UNICO, USA) at 500 nm wavelength. The pH of the solution was adjusted using dilute 0.1 N NaOH or 0.1 N HCl. To evaluate the effect of significant factors on adsorption, parameters such as pH (3–8), adsorbent dosage (0.25–1 g), contact time (5–240 min), initial phenol concentration (12–60 mg/l), and temperature (25–45°C) were investigated in batch adsorption system. Each experiment was repeated for two times and the average values were reported. The deviation lies between 0–5%.

The adsorption capacity described as the amount of adsorbate adsorbed per unit mass of adsorbent (q_e) can be expressed by the following mass balance equation:

$$q_e = \frac{(C_0 V_0 - C_e V_e)}{m} \tag{1}$$

where C_0 and C_e (mg/l) denote initial and equilibrium phenol concentration, respectively, V_0 and V_e are the volume of the solution at initial and equilibrium state, respectively (L), and m is the mass of the adsorbent (g).

The percent removal of phenol from aqueous solution was calculated by the following equation:

$$\text{Removal}\,(\%) = \frac{C_0 - C_e}{C_0} \times 100 \tag{2}$$

3. Results and discussion

3.1. characterization results

3.1.1. Elemental analysis

Table 1 presents the elemental characteristics of raw paper mill sludge. In comparison to commercial sources of activated carbon [88% carbon, 0.5% N and 3–4% ash content], sludge-based activated carbons have lower carbon content and higher ash content [25]. Among the elements, high amount of silicon is notable (30.7%). Other carbon sources such as coal, wood, or coke, usually have negligible amount of silicon [9].

Table 1
Characteristics of the paper mill sludge

Elements	Percentage (wt.%)
C	44.8
N	0.4
P	0.054
Ca	1.25
Si	30.7
Mg	0.17
Moisture	0.33
Ash	36.4

3.1.2. SEM

Scanning electron microscopy (SEM) was used to determine surface morphology of activated carbon derived from paper mill sludge. Fig. 1 shows SEM micrographs of activated carbon at 500 and 1,000 times magnification. Numerous pores with different shapes and sizes can be observed. It is clear from Fig. 1 that some particles were trapped in the pores which might block the entry of the pores (red circles). Following a series of washing steps, the adsorption capacity of the activated carbon increased due to the pore development [9].

3.1.3. FTIR

Fig. 2 shows the FTIR spectrum of the paper mill sludge-derived activated carbon. At 3,424 cm^{-1}, the broad and flat band associated with the hydroxyl group can be attributed to the adsorbed water. The weak absorption peak at 2,350 cm^{-1} is probably due to the $C\equiv C$ stretching vibration. Another shoulder which was observed at 1533 cm^{-1} can be assigned to the C=C stretching vibration [26]. The sharp and strong bond distinguished at 911 cm^{-1} is ascribed to either Si–O–C or Si–O–Si structures [27], which can be attributed to the remaining Si content in the derived activated carbon. Sharp bonds appeared in the region of 450–750 cm^{-1} is assigned to the in-plane and out-of-plane aromatic ring deformations vibrations. The peak located at 583 cm^{-1} is attributed to the out-of-plane C–H binding mode [28].

3.1.4. BET

Table 2 gives BET surface area (S_B), micropore surface area (S_m), total pore volume (V_t), micropore volume (V_m), and mean pore diameter (D_p) of the activated carbon derived from paper mill sludge. According to the definition of International Union of Pure and Applied Chemistry (IUPAC) adsorbent pores are classified into three groups: (i) micropores (<2 nm), mesopores (2–50 nm), and macropores (>50 nm). The analysis indicated that the majority of the pores fall in the range of mesopores (2–50 nm). The mean pore diameter (D_p) was calculated as $D_p = 4V_t/S_B$ [29]. In addition, the BET surface area of some synthesized activated carbon is given in Table 3.

3.2. Adsorption results

3.2.1. The effect of pH

The pH of the solution is a significant factor, because it can change the reaction kinetics and equilibrium characteristics of the adsorption process due to the variation in the degree of ionization of different pollutants [31].

In order to study the effect of solution pH on the removal and adsorption capacity of paper mill sludge-based activated carbon, experiments were performed at 25°C and phenol initial concentration of 50 mg/l at

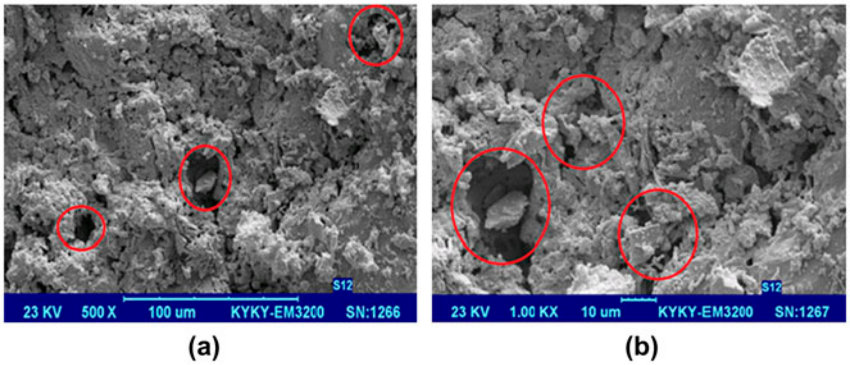

(a)

(b)

Fig. 1. SEM micrographs of activated carbon (a) surface morphology at 500 times magnification and (b) surface morphology in 1,000 times magnification.

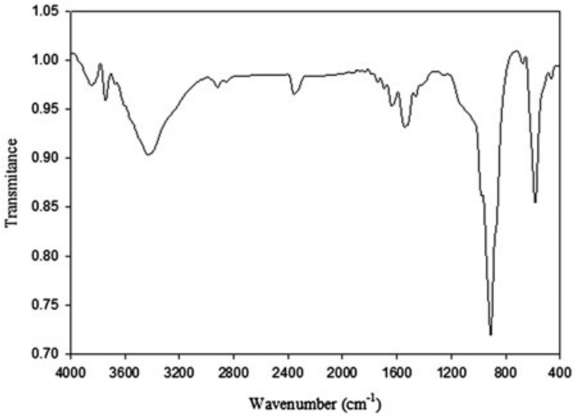

Fig. 2. FTIR spectrum of the activated carbon from paper mill sludge.

Table 2
Surface area and porosity of the developed activated carbon

S_B (m^2/g)	S_m (m^2/g)	V_t (cm^3/g)	V_m (cm^3/g)	D_p (nm)
316.32	230.1	0.4843	0.4357	6.124

different initial pH values, varied from 3 to 8. Fig. 3 shows that the adsorption capacity increased as pH of the solution was increased from 3 to 7 and then decreased as the pH increased to above 8. The isoelectric point of activated carbon is between 1 and 3 [32] which mean that at pH below 3, the overall surface charge of the activated sludge is predominantly positive and as the pH of the solution rises, the surface charge becomes negative. In acidic range (3–6), the positive surface charge of activated carbon led to interaction between aromatic ring of phenol which is activated by –OH and the carbonyl oxygen group on the surface of activated carbon according to the donor–acceptor complexation mechanism [33]. As the pH increased, the surface charge became negative and the adsorption decreased. It can be observed from Fig. 3 that the activated carbon showed the highest adsorption capacity at pH 6–7, because undissociated species of phenol is preferred by the negative functional groups on the surface. At pH higher than 8, on one hand, the solution contains phenolate ions and, on the other hand, the surface charge of the activated carbon is negative. So, the repulsion between the phenolate ions and the surface charge causes a drop in activated carbon adsorption capacity. Similar observation was reported by other researchers worked on adsorption of phenol by some kinds of activated carbons [34].

3.2.2. Adsorbent dosage

Adsorbent dosage is one of the parameters that strongly affect the adsorption capacity for a given adsorbate concentration and also determines adsorbent–adsorbate equilibria. The effect of adsorbent dosage was investigated in the range of 1.67–6.67 g/l. An increase in adsorbent dosage caused increase in phenol removal due to greater availability of the exchangeable sites on the adsorbent surface, but the specific surface area of adsorption decreased because of partial aggregation or overlapping of activated carbon [3]. As can be seen from Fig. 4, after a certain dosage phenol removal did not change noticeably. Therefore, the optimum adsorbent dosage was found where the plot of adsorption capacity and removal percent versus adsorbent dosage intersected each other. Hence, in this study, the optimum adsorbent dosage was chosen as 3 g/l (0.45 g/150 ml).

3.2.3. Effect of contact time and initial concentration

Fig. 5 presents the effect of contact time on phenol adsorption at various initial concentrations (12–60 mg/l) at 25˚C. A significant portion of phenol was removed at the first 20 min due to plenty of vacant (uncovered) adsorption sites available on the adsorbent surface. After that, the rate of adsorption became slow due to saturation of active sites. It is obvious that more time was required to reach equilibrium for the solution with higher concentration of phenol. This can be explained by knowing that adsorption of solute from a solution by porous adsorbents follows three sequential steps [35]. At first, the adsorbate transfers through the solution to the surface of the particle (film

Table 3
Comparison of BET characteristics and adsorption capacity of different low cost activated carbons

Adsorbent	BET (m^2/g)	V_t (cm^3/g)	D_p (μm)	Adsorption capacity (mg/g)
Petroleum coke [30]	96.44	0.6723	0.5205	6.01
Coal [30]	135.30	0.6081	0.353	13.23
Rice husk char [30]	230.09	1.0807	0.3836	7.91
This study	316.32	0.4843	6.124	15.04

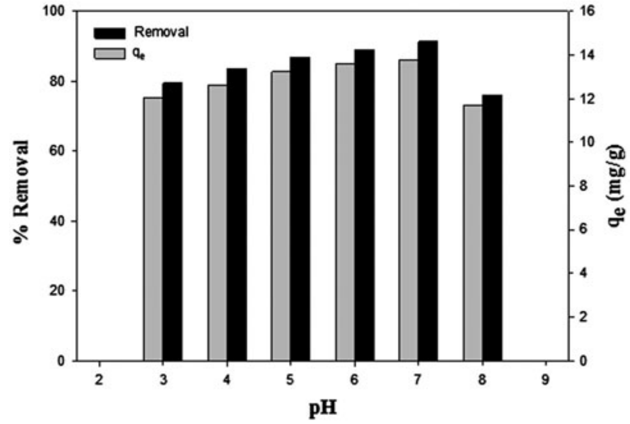

Fig. 3. Effect of solution pH on adsorption of phenol onto activated sludge ($C_0 = 50$ mg/l, adsorbent dosage = 3 g/l, T = 25°C).

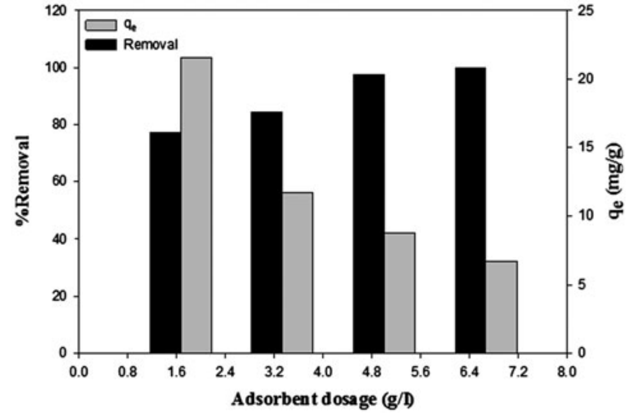

Fig. 4. Effect of adsorbent dosage on phenol removal ($C_0 = 50$ mg/l, pH = 6–7, T = 25°C).

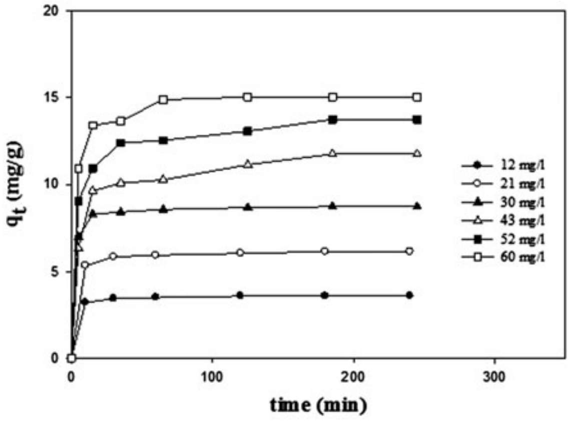

Fig. 5. Effect of contact time on phenol adsorption at different initial concentrations (adsorbent dosage = 3 g/l pH = 6–7, T = 25°C).

diffusion), then it moves into the interior site by pore diffusion and eventually it is adsorbed into the active sites at the interior surface of the adsorbent particle [36]. The transfer of solute from the solution to the surface of adsorbent (the first step) at higher concentration is encountered with stronger resistance and therefore, the time required to reach equilibrium is increased. However, total contact time chosen in this study (3 h) was sufficient to establish equilibrium for all concentrations within the range.

As the initial concentration increased from 12 to 60 mg/l, the adsorption capacity increased from 3.58 to 15.08 mg/g while the phenol removal efficiency decreased from 99.21 to 79.45%, since at higher concentrations the available active sites decreased due to competition of phenol ions for occupying these sites.

3.2.4. Adsorption isotherms

The adsorption isotherm describes how molecules of adsorbate are partitioned between adsorbent and aqueous solution at equilibrium as a function of concentration [37]. In this study, to find a relationship between the amount of phenol adsorbed onto the adsorbent and its equilibrium concentration, three isotherm models, i.e. Langmuir, Freundlich, and Langmuir–Freundlich were used.

The Langmuir isotherm model supposes a monolayer adsorption of adsorbate on the homogeneous surface and no interactions between adsorbate molecules on the adjacent sites. The non-linear form of Langmuir isotherm equation can be expressed by the following equation:

$$q_e = \frac{q_{\max} K_L C_e}{1 + K_L C_e} \tag{3}$$

where C_e is the equilibrium concentration (mg/l) and K_L (l/mg) is the Langmuir adsorption constant which is related to the energy of adsorption. $q_{\max}$ (mg/g) is the maximum adsorption capacity under experimental conditions. The essential characteristic of the Langmuir isotherm can be defined by the dimensionless parameter (R_L) which describes type of pattern; it means that the adsorption system is favorable or unfavorable [38]:

$$R_L = \frac{1}{1 + K_L C_0} \tag{4}$$

where C_0 is a highest initial phenol concentration (mg/l). When $R_L = 0$, the adsorption process is considered irreversible, favorable when $0 < R_L < 1$, linear when $R_L = 1$, and unfavorable when $R_L > 1$.

In contrast to Langmuir isotherm, Freundlich isotherm assumes a multilayer adsorption of adsorbate on heterogeneous active sites with different energies. The Freundlich isotherm is given as follows:

$$q_e = K_F C_e^{1/n} \tag{5}$$

where K_F is adsorption capacity of the adsorbent (mg/g (l/mg)$^{1/n}$) and represents bond energies between phenol ion and the adsorbent.

Langmuir–Freundlich isotherm is a combination of Langmuir and Freundlich isotherm which is used to predict heterogeneous adsorption [39]. At high concentration, the Langmuir–Freundlich isotherm reduces to Langmuir isotherm which predicts a monolayer adsorption while at low concentration, it reduces to Freundlich isotherm. Predominantly, the equation parameters are governed by operating conditions such as pH, temperature, and concentration [40].

This equation can be expressed as follows:

$$q_e = q_{\max} \frac{(K_L C_e)^b}{1 + (K_L C_e)^b} \tag{6}$$

where K_L (m^3/mg) is the equilibrium constant of Langmuir–Freundlich isotherm and is the heterogeneity factor.

The model with three fitting parameters is more suitable to fit experimental data than the Langmuir or Freundlich model. As mentioned before, b is related to the surface heterogeneity. Values higher than 0.5 may suggest that the adsorption sites can be considered similar in phenol adsorption capability. As b value reaches to unity, Langmuir–Freundlich model reduces to the Langmuir model. Fig. 6 shows three isotherm models along with experimental data at 25, 35, and 45°C.

The parameters recovered from non-linear fit of equilibrium data to the model equation for the three isotherm models are listed in Table 4. At all temperatures, the value of R_L was between 0 and 1 and this proved that the adsorption can be presumed favorable for phenol adsorption on paper mill sludge-based activated carbon under condition employed in this study [38].

The comparison of correlation factor (R^2) values shows that the best fit was obtained with the Langmuir–Freundlich isotherm.

The values of $q_{\max}$ show that the adsorbent has the capability to adsorb more phenol molecules than the amount adsorbed at the equilibrium. In other words, this model can predict the adsorption behavior at the saturation limit [41,42].

The capability of the developed activated carbon from the paper mill sludge is quite comparable with the activated carbon prepared from other waste carbonaceous materials as well as non-carbonaceous ones. The actual capacity attained by the new adsorbent at the initial phenol concentration of 40 mg/l was 11.5 mg/g of adsorbent while the activated carbon derived from pistachio shells and chemically activated by H_3PO_4 showed the adsorption capacity of about 5 mg/g of adsorbent [1]. Also, non-carbonaceous

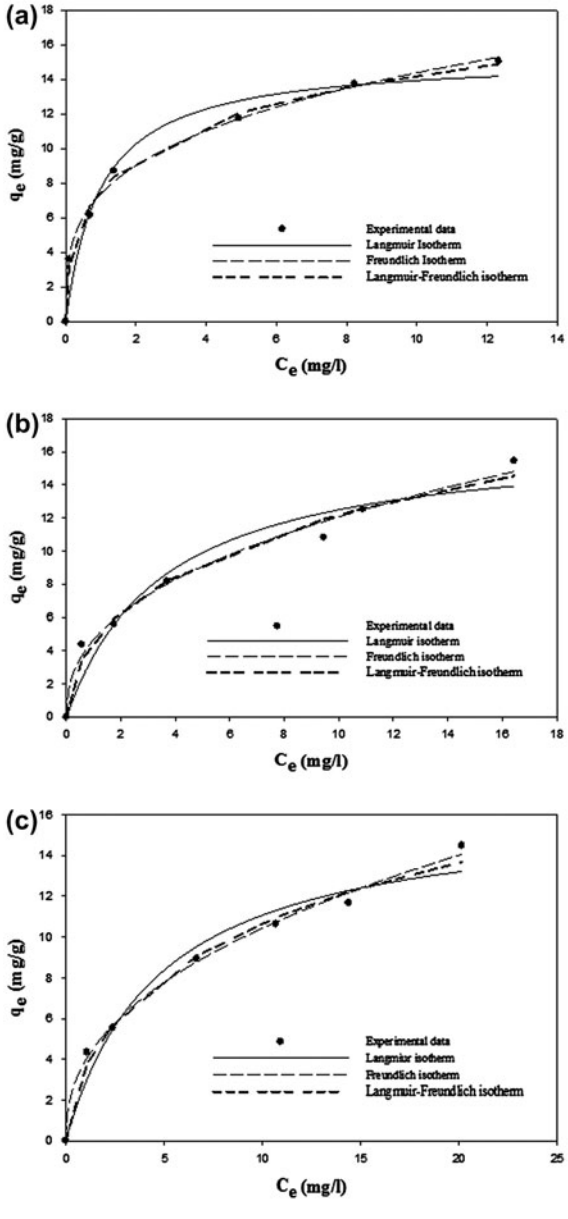

Fig. 6. Langmuir, Freundlich, and Langmuir–Freundlich isotherms for adsorption of phenol onto the activated carbon derived from paper mill sludge at (a) 25°C (b) 35°C and (c) 45°C (adsorbent dosage = 3 g/l, pH = 6–7).

Table 4
Isotherm constants for the adsorption of phenol on paper mill sludge-based activated carbon

Isotherm	Parameters value		
	25℃	35℃	45℃
Langmuir			
$q_{\max}$ (mg/g)	15.5859	16.9319	16.3449
K_L (l/mg)	1.0185	0.282	0.2102
R_L	0.016	0.052	0.0672
R^2	0.9621	0.9455	0.9693
Freundlich			
K_F ((mg/g)(l/mg)$^{1/n}$)	7.3781	4.6841	3.9211
N	3.534	2.432	2.351
R^2	0.996	0.9883	0.9961
Langmuir–Freundlich			
$q_{\max}$ (mg/g)	44.47	41.92	28.82
$K_{L,F}$ (l/mg)	0.0135	0.0182	0.0422
B	0.372	0.524	0.613
R^2	0.9984	0.991	0.9952

materials such as polymeric adsorbent demonstrated much lower adsorption capacity for phenol, between 1.5 and 3.0 mg/g of adsorbent using different types of polymers [5]. Table 3 shows the adsorption capacity of some low cost adsorbents used for phenol adsorption.

3.2.5. Adsorption kinetics

The kinetics of the adsorption explains the variation in uptake of an adsorbate in terms of time [43]. The kinetic parameters give important information for designing and modeling adsorption processes. To investigate the adsorption mechanism and determining kinetic parameters, adsorption data were analyzed using pseudo-first-order [44], pseudo-second-order, and intraparticle diffusion models [45,46].

The pseudo-first-order equation which is based on solid capacity can be expressed as follows:

$$q_t = q_e(1 - \exp(-k_1 t)) \tag{7}$$

where q_t and q_e (mg/g) are the phenol adsorption capacities at any time and at the equilibrium state (min), respectively. Also, k_1 (1/min) is the adsorption rate constant of pseudo-first-order reaction. With respect to the similarity among the data, the plot of q_t vs. t at 25℃ is typically shown in Fig. 7. The parameters of kinetic model at 25, 35, and 45℃, recovered from non-linear fit of transient adsorption data to Eq. (7), have been listed in Table 5.

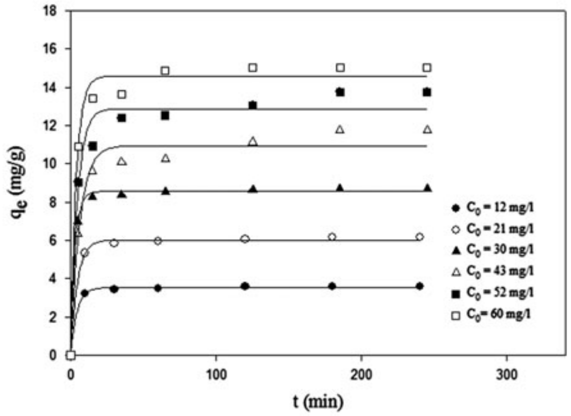

Fig. 7. Pseudo-first-order kinetic for adsorption of phenol onto the activated carbon derived from the paper mill sludge at 25℃ (adsorbent dosage = 3 g/l, pH = 6–7).

Table 5
Pseudo-first-order constants for phenol adsorption at 25, 35, and 45℃

Temperature			Pseudo-first-order model		
(℃)	C_0 (mg/l)	$q_{e,exp}$ (mg/g)	$q_{e,cal}$ (mg/g)	k_1 (1/min)	R^2
25	12	3.58	3.53	0.24	0.9983
	21	6.14	6.02	0.21	0.9978
	30	8.71	8.56	0.34	0.9978
	43	11.74	10.96	0.16	0.9757
	52	13.75	12.89	0.22	0.9711
	60	15.04	14.58	0.26	0.9868
35	15	4.38	4.22	0.30	0.997
	20	5.61	5.55	0.27	0.9972
	30	8.18	7.85	0.29	0.9831
	44	10.81	10.46	0.20	0.9724
	50	12.51	11.97	0.32	0.9843
	64	15.45	14.92	0.33	0.9926
45	15	4.33	4.21	0.29	0.9939
	20	5.52	5.39	0.23	0.9922
	35	8.92	8.83	0.33	0.9984
	44	10.63	10.39	0.28	0.9948
	51	11.67	11.47	0.18	0.994
	66	14.48	14.47	0.25	1

As can be seen from Table 5, there is a difference between experimental uptake and the predicted values by pseudo-first-order equation. Also, at 25 and 35°C, in some concentrations R^2 values are poor and do not fit the experimental data well. Some researchers also reported that the pseudo-first-order equation does not fit well the adsorption data in the whole range of contact time and is generally suitable for initial stage of adsorption [47].

The pseudo-second-order equation examined in this study can be expressed as follows:

$$q_t = \frac{k_2 q_e^2}{1 + k_2 q_e t} t \tag{8}$$

where k_2 (g/mg h) is the adsorption rate constant of pseudo-second-order reaction.

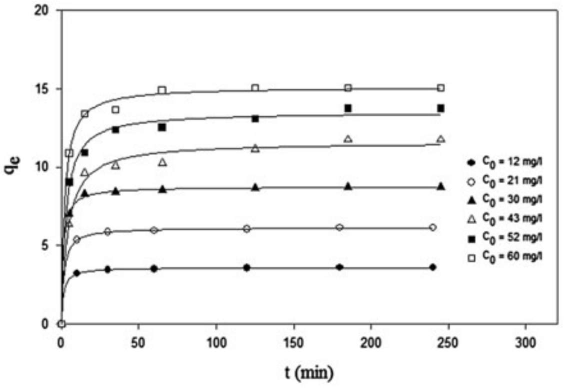

Fig. 8. Pseudo-second-order kinetic for adsorption of phenol onto the activated carbon derived from the paper mill sludge at 25℃ (adsorbent dosage = 3 g/l, pH = 6–7).

Table 6
Pseudo-second-order constants for phenol adsorption at 25, 35, and 45℃

Temperature			Pseudo-second-order model		
(℃)	C_0 (mg/l)	$q_{e,exp}$ (mg/g)	$q_{e,cal}$ (mg/g)	k_1 (g/mg min)	R^2
25	12	3.58	3.59	0.22	0.9998
	21	6.14	6.15	0.11	0.9997
	30	8.71	8.75	0.09	0.9994
	43	11.74	11.79	0.021	0.9904
	52	13.75	13.5	0.021	0.9939
	60	15.04	15.11	0.03	0.9972
35	15	4.38	4.44	0.15	0.9992
	20	5.61	5.71	0.10	0.9988
	30	8.18	8.11	0.06	0.9953
	44	10.81	10.96	0.03	0.9952
	50	12.51	12.32	0.05	0.9965
	64	15.45	15.31	0.05	0.9985
45	15	4.33	4.33	0.13	0.9996
	20	5.52	5.61	0.07	0.9999
	35	8.92	9.03	0.09	0.9993
	44	10.63	10.72	0.05	0.9992
	51	11.67	12.01	0.02	0.9976
	66	14.48	14.89	0.04	0.9931

Similarly, experimental data were tested with pseudo-second-order equation and the result for 25℃ is shown in Fig. 8.

From Table 6, it can be understood that the pseudo-second-order kinetic model has higher correlation coefficient than the pseudo-first-order model (close to unity) and the amounts of phenol uptake which is predicted by the model are in a good agreement with the experimental data.

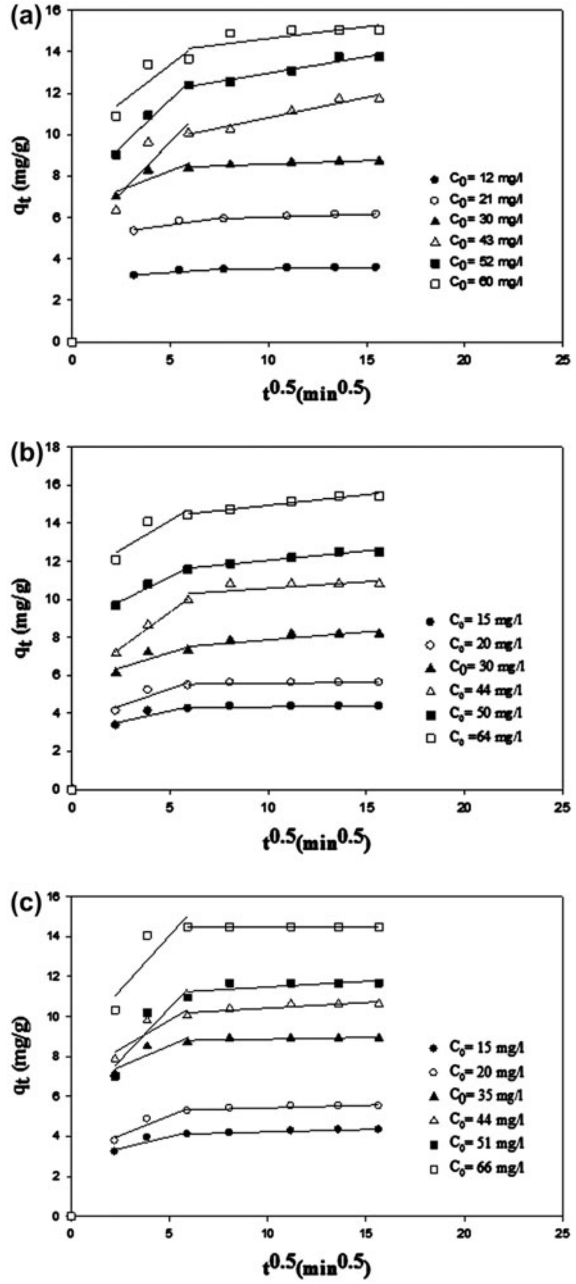

Fig. 9. Intraparticle diffusion plots for the adsorption of phenol onto the activated carbon derived from the paper mill sludge 25℃ (b) 35℃ (c) 45℃ (adsorbent dosage = 3 g/l, pH = 6–7).

3.2.6. Intraparticle diffusion model

Since pseudo-first order and pseudo-second order cannot identify the diffusion mechanism solely, the kinetic data were analyzed by the intraparticle diffusion model to explain the diffusion mechanism. This model is expressed as follows:

$$q = k_i t^{0.5} + c \tag{9}$$

where q is the amount of phenol adsorbed (mg/g) at time t, k_i is the intraparticle constant (mg/g min$^{0.5}$), and c is the intercept. The value of c gives information about the thickness of the boundary layer. It means that as the c value becomes greater, the effect of boundary layer would be higher.

The amount of phenol adsorbed vs. $t^{1/2}$ for the intraparticle transport of phenol at different concentrations and temperatures is shown in Fig. 9(a)–(c).

From this figure, it can be understood that the process involves three steps. The first and sharper portion step (line not shown for the clarity of the picture) can be attributed to mass transfer of phenol onto the external boundary layer. The second portion shows the gradual adsorption in which intraparticle is rate-limiting, while the third one indicates an equilibrium process in which the adsorption process reaches to plateau form [48]. In the stage where the intraparticle diffusion is rate-controlling, the rate of uptake might be controlled by the size of the adsorbate molecule, its concentration and its affinity to the adsorbent, and the pore size distribution of the adsorbent [49]. Table 7 lists the intraparticle constants based on Eq. (9). For all initial concentrations and temperatures, k_i for the first step was higher than k_i for the second one, while the c constant for the second part was greater than the first part. This means that at the beginning of the process, phenol removal was higher due to the large surface area available for the adsorption of phenol. After the phenol molecules aggregated on the surface of the adsorbent, the capability of the activated carbon decreased and the transportation of the phenol from exterior to the interior sites of the activated carbon particles controlled the uptake rate [29]. It is clear from Fig. 9 that the plot did not pass through the origin which indicated that intraparticle diffusion was not the only rate-controlling step; however, it played role in adsorption process.

3.2.7. Thermodynamic studies

In order to find out whether the adsorption process occurs spontaneously, both energy and entropy factors must be considered [50]. Essential thermodynamic parameters that determine the type

Table 7
Intraparticle diffusion model constants and correlation coefficients for phenol adsorption onto paper mill sludge-based activated carbon

Temperature (℃)	Intraparticle diffusion model constants						
	C_0 (mg/l)	$k_{i,1}$ (mg/g min$^{0.5}$)	$k_{i,2}$ (mg/g min$^{0.5}$)	C_1	C_2	$(R_1)^2$	$(R_2)^2$
25	12	0.06	0.01	3.03	3.4181	0.90	0.7738
	21	0.13	0.03	4.98	5.7172	0.86	0.9334
	30	0.36	0.033	6.42	8.2464	0.76	0.8891
	43	0.98	0.20	4.74	8.8538	0.79	0.9504
	52	0.90	0.16	7.17	11.3748	0.98	0.9496
	60	0.72	0.12	9.74	13.4635	0.77	0.5769
35	15	0.23	0.0119	2.98	4.22	0.80	0.4905
	20	0.36	0.0111	3.51	5.46	0.84	0.4905
	30	0.32	0.0837	5.62	7.03	0.77	0.7727
	44	0.75	0.0687	5.58	9.89	0.99	0.4905
	50	0.51	0.0997	8.6	11.05	0.97	0.96
	64	0.61	0.1118	11.07	13.83	0.81	0.9554
45	15	0.23	0.02	2.81	3.98	0.85	0.9476
	20	0.39	0.03	3.06	5.17	0.89	0.7799
	35	0.42	0.02	6.44	8.71	0.80	0.4905
	44	0.57	0.06	6.94	9.86	0.79	0.7678
	51	1.04	0.06	5.21	10.91	0.85	0.4905
	66	1.09	-1.46×10^{-16}	8.59	14.48	0.77	1

Table 8
Thermodynamic parameters for phenol adsorption on paper mill sludge-based activated carbon at different temperatures and concentrations

C_0 (mg/l)	ΔH° (kJ/mol)	ΔS° (j/mol K)	ΔG° (kJ/mol)			R^2
			25℃	35℃	45℃	
30	−62.341	−185.67	−4.14	−3.27	−2.46	0.9673
43	−36.054	−104.74	−5.06	−3.31	−2.99	0.8893
50	−29.133	−83.89	−7.51	−5.02	−3.82	0.9997

of sorption process are changes in Gibbs free energy (ΔG°), changes in enthalpy (ΔH°), and changes in entropy (ΔS°) due to transfer of unit mole of phenol from the bulk phase to the adsorbent–solution interface [51]. The Gibbs free energy can be calculated using the following equation [52]:

$$\Delta G^\circ = -RT \ln K \tag{10}$$

where R (8.314 J/mol K) is the universal gas constant and T (K) is the absolute solution temperature, and K is the adsorption equilibrium constant.

Adsorption enthalpy values were determined by the following well-known procedure based on the application of Van't Hoff equation to the equilibrium adsorption [53]:

$$\frac{\partial \ln K}{\partial T} = \frac{\Delta H^\circ}{RT^2} \tag{11}$$

After integrating and determining the constant, enthalpy changes can be expressed by the following equation

$$\ln K = \frac{\Delta S^\circ}{R} - \frac{\Delta H^\circ}{RT} \tag{12}$$

As can be seen from Eq. (12), both terms on the right side of the equation are dimensionless, so K should be dimensionless. Indeed K is partition coefficient and can be correctly described by the following equation [54,55]:

$$K = \frac{C_{\text{ads}}}{C_{\text{e}}} = \frac{C_0 - C_{\text{e}}}{C_{\text{e}}} \tag{13}$$

where C_{ads} (mg/g) is the amount of phenol adsorbed by the adsorbent. Thus, the K value for some phenol concentrations was calculated at different temperatures. ΔH° and ΔS° were calculated from the slope and the intercept of Van't Hoff plots, respectively. The obtained thermodynamic parameters and correlation coefficient (R^2) have been listed in Table 8. These parameters determine the orientation and feasibility of physiochemical adsorptive reaction [56]. The negative values of the Gibbs free energy in at all temperatures demonstrated that the phenol adsorption was thermodynamically spontaneous. As can be seen from Table 8, ΔG° values decreased with increase in temperature which means that adsorption was not favorable at higher temperatures [57]. Sign of enthalpy change of adsorption gives useful information whether total energy is consumed/released in bonding adsorbate–adsorbent. The negative values of ΔH° indicated that the adsorption process was exothermic. In general, the adsorption with ΔH° values in the range of 2.1–20.9 and 80–200 kJ/mol can be considered as physical and chemical adsorption, respectively [57]. In this study, the values of ΔH° revealed that the adsorption of phenol on the paper mill sludge-based activated carbon was dominated by physisorption mechanism. Sign of entropy change of adsorption describes randomness of the adsorption at the adsorbate–adsorbent interface. A negative value of ΔS° is an indicator of decrease in randomness of bonding between adsorbate and adsorbent at the interface. The adsorption entropy changes were negative which can be justified by the fact that the mobility of phenol on the activated carbon surface becomes more restricted compared to their mobility in the solution [58]. Therefore, the adsorption process which was performed under mentioned conditions is considered as enthalpy-driven process [50].

3.2.8. Activation energy

Phenol adsorption on activated carbon can be evaluated by Arrhenius equation which relates rate constant to the temperature as follows:

$$k_2 = A \exp\left(-\frac{E_{\text{a}}}{RT}\right) \tag{14}$$

where k_2 is the rate constant (g/mg.min) calculated from pseudo-second-order rate constant at operational

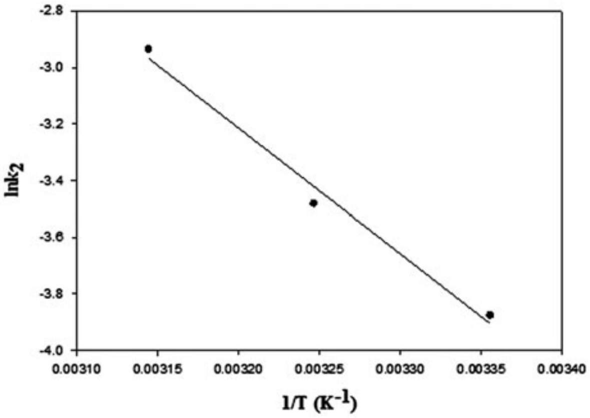

Fig. 10. Determination of activation energy for phenol adsorption onto the activated carbon derived from the paper mill sludge.

Table 9
Arrhenius constants for phenol adsorption onto the activated carbon derived from the paper mill sludge

A (g/mg min)	E_a (kJ/mol)	R^2
60,475	36.95	0.9876

temperatures, A is Arrhenius constant (g/mg min) and E_a is activation energy (kJ/mol).

Linear form of Eq. (14) is represented by the following equation:

$$\ln k_2 = \ln A - \frac{E_a}{RT} \tag{15}$$

where parameters E_a and A can be determined from the slope and the intercept of the line (Fig. 10). The value of the activation energy is commonly used to find the type of adsorption process. In physical adsorption, reactions are reversible, reach equilibrium quickly, and require low amount of energy ranging from 5 to 40 kJ/mol while in chemical adsorption, reactions comprise of strong forces and require high amount of activation energy ranging from 40 to 800 kJ/mol [59,60]. In this study, the activation energy obtained for adsorption of phenol on activated carbon was 36.95 kJ/mol suggesting that the adsorption of phenol occurred physically. Other parameters are summarized in Table 9.

4. Conclusion

A new activated carbon was synthesized from the digested paper mill sludge and was used as an adsorbent for removing phenol from aqueous solution. The produced activated carbon was found to have a mesoporous surface with remarkable surface area (316 m^2/g). SEM micrograph demonstrated a porous surface with numerous pores with different shapes and sizes. FTIR spectrum indicated the presence of some surface functional groups such as C=C and Si–C–O, or Si–C–Si. The results showed that the adsorption capacity was affected by solution pH and the optimal solution pH was in the range of 6–7. Also, it was observed that as the temperature increased, the adsorption capacity decreased. Thus, maximum capacity was obtained at 25°C with 15.04 mg/g. The Langmuir, Freundlich, and Langmuir–Freundlich isotherm models were used to express the adsorption of phenol onto the paper mill sludge-based activated carbon. The results indicated that the Langmuir–Freundlich isotherm fitted the experimental data well. The pseudo-first order and pseudo-second order were employed to study the kinetics of the phenol sorption. The results showed that pseudo-second order provided better correlation for the adsorption data and it was observed that intraparticle diffusion was not the only rate-controlling step. According to the enthalpy values, the type of adsorption of phenol onto the paper mill sludge-based activated carbon was defined as a physical adsorption and the process was exothermic. The negative values of ΔG° showed that the adsorption of phenol was spontaneous. As a conclusion, the paper mill sludge is an alternative potential precursor that can be used as a low cost adsorbent and would cost less than the commercial activated carbon.

References

[1] A.A. Attia, B.S. Girgis, S.A. Khedr, Capacity of activated carbon derived from pistachio shells by H3PO4 in the removal of dyes and phenolics, J. Chem. Technol. Biotechnol. 78 (2003) 611–619.
[2] M. Ahmaruzzaman, Adsorption of phenolic compounds on low-cost adsorbents: A review, Adv. Colloid Interface Sci. 143 (2008) 48–67.
[3] M. Kilic, E. Apaydin-Varol, A.E. Pütün, Adsorptive removal of phenol from aqueous solutions on activated carbon prepared from tobacco residues: Equilibrium, kinetics and thermodynamics, J. Hazard. Mater. 189 (2011) 397–403.
[4] Q. Jia, A.C. Lua, Effects of pyrolysis conditions on the physical characteristics of oil-palm-shell activated carbons used in aqueous phase phenol adsorption, J. Anal. Appl. Pyrolysis 83 (2008) 175–179.
[5] M.A. Hararah, K.A. Ibrahim, A.H. Al-Muhtaseb, R.I. Yousef, A. Abu-Surrah, A. Qatatsheh, Removal of phenol from aqueous solutions by adsorption onto polymeric adsorbents, J. Appl. Polym. Sci. 117 (2010) 1908–1913.
[6] M. Torab-Mostaedi, M. Asadollahzadeh, A. Hemmati, A. Khosravi, Equilibrium, kinetic, and thermodynamic studies for biosorption of cadmium and nickel on grapefruit peel, J. Taiwan Inst. Chem. 44 (2013) 295–302.

[7] B. Pan, W. Zhang, Q. Zhang, S. Zheng, Adsorptive removal of phenol from aqueous phase by using a porous acrylic ester polymer, J. Hazard. Mater. 157 (2008) 293.
[8] T. Altun, E. Pehlivan, Removal of Copper (II) ions from aqueous solutions by Walnut-, Hazelnut-and Almond-shells, CLEAN–Soil, Air, Water 35 (2007) 601–606.
[9] X. Chen, S. Jeyaseelan, N. Graham, Physical and chemical properties study of the activated carbon made from sewage sludge, Waste Manage. 22 (2002) 755–760.
[10] M. Otero, F. Rozada, L. Calvo, A. Garcıa, A. Moran, Elimination of organic water pollutants using adsorbents obtained from sewage sludge, Dyes Pig. 57 (2003) 55–65.
[11] O. Ioannidou, A. Zabaniotou, Agricultural residues as precursors for activated carbon production—a review, Renewable Sustainable Energy Rev. 11 (2007) 1966–2005.
[12] M.K.B. Gratuito, T. Panyathanmaporn, R.A. Chumnanklang, N. Sirinuntawittaya, A. Dutta, Production of activated carbon from coconut shell: Optimization using response surface methodology, Bioresour. Technol. 99 (2008) 4887–4895.
[13] D. Prahas, Y. Kartika, N. Indraswati, S. lsmadji, Activated carbon from jackfruit peel waste by H3PO4 chemical activation: Pore structure and surface chemistry characterization, Chem. Eng. J. 140 (2008) 32–42.
[14] V.S. Mane, P. Vijay Babu, Kinetic and equilibrium studies on the removal of Congo red from aqueous solution using Eucalyptus wood (Eucalyptus globulus) saw dust, J. Taiwan Inst. Chem. 44(2013) (2012) 81–88.
[15] E. Khoramzadeh, B. Nasernejad, R. Halladj, Mercury biosorption from aqueous solutions by Sugarcane Bagasse, J. Taiwan Inst. Chem. 44(2013) (2012) 266–269.
[16] M. Ajmal, A. Hussain Khan, S. Ahmad, A. Ahmad, Role of sawdust in the removal of copper (II) from industrial wastes, Water Res. 32 (1998) 3085–3091.
[17] S. Al-Asheh, Z. Duvnjak, Binary metal sorption by pine bark: Study of equilibria and mechanisms, Sep. Sci. Technol. 33 (1998) 1303–1329.
[18] M. Ahmedna, W.E. Marshall, A.A. Husseiny, R.M. Rao, I. Goktepe, The use of nutshell carbons in drinking water filters for removal of trace metals, Water Res. 38 (2004) 1062–1068.
[19] A.H. El-Sheikh, A.P. Newman, H.K. Al-Daffaee, S. Phull, N. Cresswell, Characterization of activated carbon prepared from a single cultivar of Jordanian Olive stones by chemical and physicochemical techniques, J. Anal. Appl. Pyrol. 71 (2004) 151–164.
[20] I. Alomá, M. Martín-Lara, I. Rodríguez, G. Blázquez, M. Calero, Removal of nickel (II) ions from aqueous solutions by biosorption on sugarcane bagasse, J. Taiwan Inst. Chem. 43 (2012) 275–281.
[21] M. Revathi, M. Saravanan, A.B. Chiya, M. Velan, Removal of Copper, Nickel, and Zinc ions from electroplating rinse water, CLEAN–Soil, Air, Water 40 (2012) 66–79.
[22] D. Fytili, A. Zabaniotou, Utilization of sewage sludge in EU application of old and new methods—a review, Renewable Sustainable Energy Rev. 12 (2008) 116–140.
[23] W.H. Li, Q.Y. Yue, B.Y. Gao, X.J. Wang, Y.F. Qi, Y.Q. Zhao et al., Preparation of sludge-based activated carbon made from paper mill sewage sludge by steam activation for dye wastewater treatment, Desalin. 278 (2011) 179–185.
[24] W.-H. Li, Q.-Y. Yue, B.-Y. Gao, X.-J. Wang, Y.-F. Qi, Y.-Q. Zhao et al., Preparation of sludge-based activated carbon made from paper mill sewage sludge by steam activation for dye wastewater treatment, Desalin. 278 (2011) 179–185.
[25] R.C. Bansal, J.B. Donnet, and F. Stoeckli, "Active carbon", M. Dekker, 1988.
[26] I. Tan, A. Ahmad, B. Hameed, Preparation of activated carbon from coconut husk: Optimization study on removal of 2, 4, 6-trichlorophenol using response surface methodology, J. Hazard. Mater. 153 (2008) 709–717.
[27] O. Duggan, S.J. Allen, Study of the physical and chemical characteristics of a range of chemically treated, lignite based carbons, Water Sci. Technol. 35 (1997) 21–27.
[28] Z. Al-Qodah, R. Shawabkah, Production and characterization of granular activated carbon from activated sludge, Braz. J. Chem. Eng. 26 (2009) 127–136.
[29] L. Wang, J. Zhang, R. Zhao, Y. Li, C. Li, C. Zhang, Adsorption of Pb (II) on activated carbon prepared from Polygonum orientale Linn: Kinetics, isotherms, pH, and ionic strength studies, Bioresour. Technol. 101 (2010) 5808–5814.
[30] M. Ahmaruzzaman, D. Sharma, Adsorption of phenols from wastewater, J. Colloid Interface Sci. 287 (2005) 14–24.
[31] N. Siva Kumar, M. Venkata Subbaiah, A. Subba Reddy, A. Krishnaiah, Biosorption of phenolic compounds from aqueous solutions onto chitosan–abrus precatorius blended beads, J. Chem. Technol. Biotechnol. 84 (2009) 972–981.
[32] Z. Aksu, D. Akpinar, Competitive biosorption of phenol and chromium (VI) from binary mixtures onto dried anaerobic activated sludge, Biochem. Eng. J. 7 (2001) 183–193.
[33] U. Beker, B. Ganbold, H. Dertli, D.D. Gülbayir, Adsorption of phenol by activated carbon: Influence of activation methods and solution pH, Energy Convers. Manage. 51 (2010) 235–240.
[34] U. Thawornchaisit, K. Pakulanon, Application of dried sewage sludge as phenol biosorbent, Bioresour. Technol. 98 (2007) 140–144.
[35] D. Faust, M. Aly, Chemistry of Wastewater Treatment, Butterworthworts, Boston, MA, 1983.
[36] B. Hameed, A. Rahman, Removal of phenol from aqueous solutions by adsorption onto activated carbon prepared from biomass material, J. Hazard. Mater. 160 (2008) 576–581.
[37] M. Momčilović, M. Purenović, A. Bojić, A. Zarubica, M. Ranđelović, Removal of lead (II) ions from aqueous solutions by adsorption onto pine cone activated carbon, Desalin. 276 (2011) 53–59.
[38] K.L. Wasewar, M. Atif, B. Prasad, I.M. Mishra, Adsorption of zinc using tea factory waste: Kinetics, equilibrium and thermodynamics, CLEAN–Soil, Air, Water 36 (2008) 320–329.
[39] A. Gunay, E. Arslankaya, İ. Tosun, Lead removal from aqueous solution by natural and pretreated clinoptilolite: Adsorption equilibrium and kinetics, J. Hazard. Mater. 146 (2007) 362–371.
[40] A. Pérez-Marín, V.M. Zapata, J. Ortuno, M. Aguilar, J. Sáez, M. Lloréns, Removal of cadmium from aqueous solutions by adsorption onto orange waste, J. Hazard. Mater. 139 (2007) 122–131.
[41] H. Jankowska, A. Świątkowski, J. Choma, T.J. Kemp, Active Carbon, Ellis Horwood, New York, 1991.
[42] M. Seredych, T.J. Bandosz, Removal of copper on composite sewage sludge/industrial sludge-based adsorbents: The role of surface chemistry, J. Colloid Interface Sci. 302 (2006) 379–388.
[43] I. Tan, A. Ahmad, B. Hameed, Adsorption isotherms, kinetics, thermodynamics and desorption studies of 2, 4, 6-trichlorophenol on oil palm empty fruit bunch-based activated carbon, J. Hazard. Mater. 164 (2009) 473–482.
[44] J. Febrianto, A.N. Kosasih, J. Sunarso, Y.H. Ju, N. Indraswati, S. Ismadji, Equilibrium and kinetic studies in adsorption of heavy metals using biosorbent: A summary of recent studies, J. Hazard. Mater. 162 (2009) 616–645.
[45] Y. Ho, G. McKay, Pseudo-second order model for sorption processes, Process Bioche. 34 (1999) 451–465.
[46] Y. Ho, G. McKay, D. Wase, C. Forster, Study of the sorption of divalent metal ions on to peat, Adsorpt. Sci. Technol. 18 (2000) 639–650.
[47] Y. Ho, G. McKay, The sorption of lead (II) ions on peat, Water Res. 33 (1999) 578–584.
[48] F.C. Wu, R.L. Tseng, R.S. Juang, Comparisons of porous and adsorption properties of carbons activated by steam and KOH, J. Colloid Interface Sci. 283 (2005) 49–56.
[49] P. Antonio, K. Iha, M. Suárez-Iha, Kinetic modeling of adsorption of di-2-pyridylketone salicyloylhydrazone on silica gel, J. Colloid Interface Sci. 307 (2007) 24–28.

[50] A. Rathinam, B. Maharshi, S.K. Janardhanan, R.R. Jonnalagadda, B.U. Nair, Biosorption of cadmium metal ion from simulated wastewaters using Hypnea valentiae biomass: A kinetic and thermodynamic study, Bioresour. Technol. 101 (2010) 1466–1470.

[51] R.I. Yousef, B. El-Eswed, A.H. Al-Muhtaseb, Adsorption characteristics of natural zeolites as solid adsorbents for phenol removal from aqueous solutions: Kinetics, mechanism, and thermodynamics studies, Chem. Eng. J. 171 (2011) 1143–1149.

[52] V.K. Gupta, I. Ali, Removal of lead and chromium from wastewater using bagasse fly ash—a sugar industry waste, J. Colloid Interface Sci. 271 (2004) 321–328.

[53] V.M. Monsalvo, A.F. Mohedano, J.J. Rodriguez, Adsorption of 4-chlorophenol by inexpensive sewage sludge-based adsorbents from sewage sludge, Chem. Eng. Res. Des. 90 (2012) 1807–1814.

[54] W. Wan Ngah, M. Hanafiah, Adsorption of copper on rubber (Hevea brasiliensis) leaf powder: Kinetic, equilibrium and thermodynamic studies, Biochem. Eng. J 39 (2008) 521–530.

[55] D. Kim, Adsorption characteristics of Fe (III) and Fe (III)–NTA complex on granular activated carbon, J. Hazard. Mater. 106 (2004) 67–84.

[56] Y.H. Li, Z. Di, J. Ding, D. Wu, Z. Luan, Y. Zhu, Adsorption thermodynamic, kinetic and desorption studies of Pb^{2+} on carbon nanotubes, Water Res. 39 (2005) 605–609.

[57] A. Sari, M. Tuzen, D. Citak, M. Soylak, Equilibrium, kinetic and thermodynamic studies of adsorption of Pb (II) from aqueous solution onto Turkish kaolinite clay, J. Hazard. Mater. 149 (2007) 283–291.

[58] K. Li, X. Wang, Adsorptive removal of Pb (II) by activated carbon prepared from Spartina alterniflora: Equilibrium, kinetics and thermodynamics, Bioresour. Technol. 100 (2009) 2810–2815.

[59] E. Unuabonah, K. Adebowale, B. Olu-Owolabi, Kinetic and thermodynamic studies of the adsorption of lead (II) ions onto phosphate-modified kaolinite clay, J. Hazard. Mater. 144 (2007) 386–395.

[60] A. Ozcan, A. Ozcan, O. Gok, Adsorption Kinetics and Isotherms of Anionic Dye of Reactive Blue 19 from Aqueous Solutions onto DTMA-Sepiolite, Hazardous Materials and Wastewater—Treatment, Removal and Analysis, Nova Science, New York, 2007.